Continuum contact process and influence of impurity on the critical behavior in absorbing-state phase transitions in two dimensions

Sang Bub Lee [*] and Jin Min Kim [†]
Department of Physics and OMEG Institute, Soongsil University, Seoul 06978, Korea

(Received 12 September 2023; accepted 22 November 2023; published 28 December 2023)

We study via Monte Carlo simulations the influence of quenched and mobile impurities in the contact process (CP) on two-dimensional lattice and continuum systems. In the lattice system, the effect of mobile impurity was studied for the density $n_i = 0.2$ and two selected values of hopping probability for impurity particles, $w = 0.5$ and 1. In the continuum system, the CP was defined by distributing spherical impurity particles of diameter σ_i and number density $n_i = 0.2$ and active particles of diameter unity and number density $1 - n_i$ on a square substrate with periodic boundaries. In each dynamic process, a particle is selected at random; the active particle either creates with a rate λ an offspring at a distance r ($1 \leqslant r \leqslant 1.5$) from the active particle or annihilates with a unit rate, and the impurity particle hops a distance r ($0 \leqslant r \leqslant 1$), both along randomly selected directions. We found that the lattice CP shows power-law behaviors with varying critical exponents depending on the values of w. For the continuum CP with quenched impurity, the critical behavior followed the activated scaling scenario, whereas with mobile impurity usual power-law behaviors were observed but the critical exponents varied depending on the values of σ_i.

DOI: 10.1103/PhysRevE.108.064135

I. INTRODUCTION

Nonequilibrium continuous phase transitions of reaction-diffusion systems have attracted considerable attention during the past decades [1–4]. The simplest model that exhibits such a transition is the contact process (CP) with a reaction-diffusion scheme of spreading $A \to 2A$ with a rate λ and extinction $A \to 0$ with a rate μ [5,6]. As λ decreases, the system undergoes a phase transition from an active phase into an inactive absorbing state at the critical rate λ_c. The CP is known to show the same critical behavior as that of models that belong to the widely known directed percolation (DP) universality class [7,8], to which various models satisfying the DP conjecture—such as the reaction-diffusion process, damage spreading, certain probabilistic cellular automata [9,10], and pair-contact process [11]—are known to belong. Different universality classes such as the parity-conserving class [12,13] and conserved DP class (also called Manna class) [14,15] were also reported for models with additional symmetries and conservation laws that were not specified in the DP conjecture.

Most models proposed so far describing the absorbing phase transition (APT) were proposed on lattices, and only few that mimic population dynamics were carried out on a continuum substrate with point particles [16,17]. It was only recently that models in continuous media with particles having excluded volume were studied to understand the experimental observations for driven colloidal suspensions [18,19]. The APT in continuous media is less interesting, because the lattice and continuum models are known to exhibit the same critical behavior in equilibrium statistical physics, and the same universality is believed to hold for nonequilibrium systems as well. However, the recently developed interacting particle model in continuous media was reported to exhibit a critical behavior that is consistent with the DP critical behavior despite an additional conservation of the number of particles [20]. More recently, one of us studied an overlapping particle model that is believed to belong to the same universality class as the interacting particle model of Ref. [20] and showed that the critical behavior was distinct from the DP critical behavior [21].

An influence of uncorrelated quenched disorder on the critical behavior in the APT was introduced by applying the Harris criterion [22], established originally for equilibrium spin systems, to the nonequilibrium APT, and has attracted great interest in recent decades. The Harris criterion implies that, for any amount of quenched disorder added to a system, the pure fixed point is unstable if the specific heat exponent $\alpha > 0$, suggesting that the critical behavior of the disordered system differs from that of the pure system. For an APT, the hyperscaling relation $\alpha = 2 - d\nu$ [23] leads the disorder to be relevant if $d\nu < 2$, where d and ν are, respectively, the substrate dimension and spatial correlation-length exponent. This problem was first studied by Kinzel [9] and later in more detail by Noest [24], who studied the critical behavior of spatially disordered stochastic cellular automata (SCA). Moreira and Dickman subsequently studied by Monte Carlo (MC) simulations the influence of random dilution of lattice sites on a two-dimensional (2D) CP [25–27]. Both the clean SCA and CP are known to belong to the DP universality class for which $d\nu < 2$ holds for $d < 4$. In these studies, quenched impurity

[*]Present address: Kyungpook National University, Daegu 41566, Korea; sblee@knu.ac.kr
[†]Corresponding author: jmkim@ssu.ac.kr

yielded spreading from a single particle on a disordered system that was logarithmic at the critical point, and the existence of the Griffiths phase between pure and disordered critical points where the time dependence is governed by nonuniversal power laws. The renormalization calculation using the Reggeon field theory also supported instability of a pure fixed point [28].

Recently Hooyberghs *et al.* further explored the effect of randomness by strong disorder renormalization-group calculations by mapping a 1D disordered CP onto a random quantum-spin chain using the Hamiltonian formalism and found that the transition is controlled by an infinite randomness fixed point [29]. At the infinite randomness fixed point, the power-law scaling $\tau \sim \xi^z$, τ and ξ being, respectively, the temporal and spatial correlation lengths, was predicted to be replaced by the activated dynamic scaling $\ln \tau \sim \xi^\psi$, ψ being the tunneling exponent, whereas the static scaling behavior remained a conventional power-law type. The activated scaling yields the density of particles and survival probability of diverging logarithmically in the asymptotes. For a weak disorder, they predicted nonuniversal exponents that vary continuously with the strength of disorder. Vojta and Dickison [30] confirmed in one dimension and Vojta, Farquhar, and Mast [31] in two dimensions by MC simulations the effect of quenched spatial disorder and showed that the critical behavior was indeed described by the infinite randomness fixed point. They also found that this behavior was universal, suggesting that it occurs even in weak disorder with the same critical exponents. A mapping of disordered CP onto random quantum magnets enables one to predict the critical behavior of disordered CP in higher dimensions. Senthil and Sachdev showed that the activated dynamic scaling observed in 1D random quantum Ising model is also observed in any dimensions $d > 1$ [32]. This prediction in four dimensions, however, contradicts the Harris criterion that suggested an ordinary power-law scaling at the upper critical dimension of $d_c = 4$ where $d\nu_\perp = 2$. We recently observed in four dimensions the usual power-law scaling when the amount of disorder is less than the percolation threshold, favoring the Harris criterion rather than the prediction by a mapping onto random quantum magnets [33].

While the influence of quenched disorder on the CP is now widely understood, the effect of mobile impurity was studied only in one dimension via numerical simulations. Dickman studied the CP on a chain with diffusing passive sites that do not participate actively and found that the critical behavior is affected; the critical exponents δ and z, the ratio $\beta/\nu_\perp$, and the moment ratio $m = \langle \rho^2 \rangle / \langle \rho \rangle^2$ take the values different from the DP values [34]. Nearly at the same time Evron, Kessler, and Shnerb carried out MC simulations for the model in which certain (good) sites having higher creation rate than others (bad sites) diffuse on the lattice, and found that the density of particles showed the power-law behavior $\rho(t) \sim t^{-\delta}$ with the same power as that of DP at the critical point [35]. At first glance, the two models appear to be identical when the creation rate at the bad sites is 0; however, there is a subtle difference. While in the latter offspring may be created on bad sites, in the former particles never sit on passive sites. Although it was not rigorously proved that this difference changes the critical behavior, the difference was considered to be irrelevant because the rate equations for the two models are equivalent [34].

One dimension is topologically different from higher dimensions. Active sites on a chain may be divided into few finite clusters when passive sites are added, and sizes of clusters may vary by the mobility of passive sites but, the active sites can never form an infinite cluster. In the CP, particles on a finite cluster eventually disappear by fluctuation as long as the creation rate is finite. Dickman avoided this situation by the prescription that, when a passive site encountered a particle by diffusion, the positions of the two were assumed to be exchanged. In two and higher dimensions, such a prescription is unnecessary because finite clusters of active sites at one time may merge to an infinite cluster at a later time by mobility of passive sites.

In this paper, we investigate by MC simulations the effect of impurity on the critical behavior for the lattice and continuum CP models in more the realistic case of two dimensions. For the lattice model, since the effect of quenched impurity has been extensively studied in recent years, we study the effect of mobile impurity to see whether the critical behavior is qualitatively similar to that in one dimension despite topological differences. For a continuum model, we propose a continuum version of the CP and examine if the new model exhibits the DP critical behaviors. We also study the effect of quenched and mobile impurity to examine if the critical behavior is qualitatively similar to that of the lattice model. The impurities are assumed to be disks that are inactive and impenetrable to each other and to active particles. Details of the model are presented in Sec. II.

For the lattice CP, the effect of the mobile impurity was found to be distinct from that for the quenched impurity but was qualitatively consistent with that in one dimension. For the continuum CP, the critical behavior of the clean CP was consistent with that of the lattice CP but was distinct from that for the interacting particle model proposed to study driven colloidal suspensions. The stationary inactive particles yielded decreasing active-particle density following the nonuniversal power laws within the region of $\lambda_c^0 < \lambda < \lambda_c$, supporting the existence of the Griffiths phase as for the disordered lattice CP. The mobile impurity, on the other hand, yielded a conventional power-law behavior with the critical exponents depending on the density of impurity particles.

In Sec. II models and simulation methods are presented and in Sec. III the numerical results with appropriate discussions are given. Concluding remarks and possible application of the continuum model are presented in Sec. IV.

II. MODELS AND SIMULATION METHODS

The clean CP has two processes: creation of offspring (spreading) with a rate λ and annihilation (extinction) with a rate μ (set to be $\mu = 1$). The MC simulations were carried out probabilistically with creation probability $p_\lambda = \frac{\lambda}{1+\lambda}$ for spreading and annihilation probability $p_\mu = \frac{1}{1+\lambda}$ for extinction using two different ways of updates: parallel and sequential updates. Sequential updates are employed through out the paper.

CP with mobile impurity on a lattice. When an impurity is added to the system, the simulation of CP on a lattice is carried

out as follows. Initially $n_i L^2$ randomly selected sites are filled with impurity particles and the remaining $\rho_0 L^2$ sites are filled with active particles on an $L \times L$ square lattice with periodic boundaries, i.e., $n_i + \rho_0 = 1$. In each update procedure, a particle is selected at random. (i) If the particle is active, spreading or extinction is determined as for the clean CP. If spreading is chosen, a nearest-neighbor (nn) site is selected at random, and a new active particle is created on the nn site if it is empty and nothing happens otherwise. If extinction is chosen, the particle is removed from the system. The evolution time is increased by an amount $\Delta t = \frac{1}{\rho(t)L^2}$, where $\rho(t)$ is the density of active particles at time t. The datum of $\rho(t)$ is saved whenever the accumulated time exceeds an integer value. (ii) If the particle is an impurity particle, an nn site is selected at random and the particle hops to the nn site with probability w when the nn site is empty. If the nn site is filled with a particle, the selected particle stays on its position. It should be noted that the evolution time is increased only for case (i); however, it can be updated alternatively by an amount of $\Delta t = \frac{1}{(\rho(t)+n_i)L^2}$ for both cases (i) and (ii). The results should remain the same.

CP in continuous media. In continuous media, the clean CP is designed as follows. Initially L^2 particles of a diameter unity ($\sigma = 1$) are distributed on the lattice sites, and each particle either creates an offspring with a rate λ or annihilates with a unit rate. (Note that the diameter of active particles is the unit of length through out the paper.) When an offspring is to be created, it is not necessarily created on the lattice sites but anywhere at a distance r from the center of the mother particle. For convenience sake, we choose $1 \leqslant r \leqslant 1.5$. If the position of offspring i is overlapped with any of the existing particles j, i.e., if $|\mathbf{r}_i - \mathbf{r}_j| < 1$, $\mathbf{r}_i$ and $\mathbf{r}_j$ representing the position vectors of the centers of particles i and j, respectively, the creation is abandoned. The continuum CP is similar to the lattice CP and, therefore, the two models are expected to belong to the same universality class.

Continuum CP with impurity. When an impurity is added, we assume that impurity is of the form of disks of diameter σ_i and number density n_i which are impenetrable to both active and impurity particles. When the impurity is quenched, $n_i L^2$ impurity particles and $\rho_0 L^2$ active particles are distributed on randomly selected positions in the $L \times L$ square substrate. (We here chose $\rho_0 = 1 - n_i$ for consistency with other cases.) In each process, one of the active particles is selected and spreading or extinction is determined probabilistically. When spreading is chosen, the new position $\mathbf{r}$ is selected at random within a distance $1 < r < 1.5$, as shown in Fig. 1. Creation of a new particle centered at $\mathbf{r}$ is accepted if $|\mathbf{r} - \mathbf{r}_j| > \frac{1+\sigma_j}{2}$, $\mathbf{r}_j$ and σ_j being, respectively, the position vector and diameter of the existing nearby particles, otherwise it is abandoned. When extinction is chosen, the particle is removed from the system. Assuming the universality between continuum and lattice CP, the data of $\rho(t)$ are expected to show a nonuniversal power-law behavior in the region of $\lambda_c^0 < \lambda < \lambda_c$ and activated scaling at λ_c, where λ_c^0 and λ_c are the critical spreading rates of the clean and dirty (with impurity) systems, respectively. We will qualitatively examine if the system exhibits such behaviors in the continuum CP.

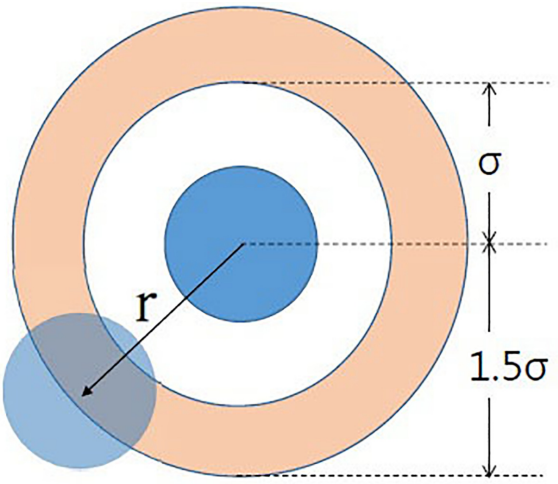

FIG. 1. Spreading of an offspring (light blue disk) within the region (light orange shell) of a distance r, $\sigma \leqslant r \leqslant 1.5\sigma$ ($\sigma = 1$), from the center of the mother particle (blue disk). This guarantees that the offspring avoids overlapping with its mother particle.

When the impurity is annealed or impurity particles are mobile, initially $n_i L^2$ impurity particles are distributed on randomly selected lattice sites and $\rho_0 L^2$ active particles on the remaining sites. In the next and forthcoming steps, one of the $[\rho(t) + n_i]L^2$ particles is selected at random. It should be noted that the density of active particles varies as time evolves from the initial density ρ_0 to $\rho(t)$ at time t, whereas impurity-particle density remains constant. When an active particle is selected, the spreading or extinction proceeds by the same way as for the CP with quenched impurity. When an impurity particle is selected, it hops to a new position at a distance r within $0 < r < 1$ if the new position does not overlap with any of the nearby particles, otherwise it stays on its position. Although the dynamics begins with particles on lattice sites, they will be anywhere in the system after a transient time. When the impurity is annealed, the Harris criterion is no longer applicable, and the ideal critical exponents for equilibrium systems were known to be given by the Fisher renormalization [36]. We will investigate whether the mobile impurity affects the critical behavior of the continuum CP.

Since our primary purpose is to examine how the mobility of impurity influences the critical behavior of the APT, it is necessary to vary the density of impurity particles and hopping probability, the latter of which is associated with the velocity of impurity particles. The number density of impurities is fixed to be $n_i = 0.2$ for both lattice and continuum CP, so the simulation begins with 8×10^5 impurity particles and 3.2×10^6 active particles on a system of linear size $L = 2000$. The two values of hopping probability, $w = 0.5$ and 1.0, are selected for the lattice model to qualitatively investigate the effect of velocity on the critical behavior. For the continuum CP, the density of the impurity is associated with the excluded area of occupation for active-particle centers, which can be varied by varying n_i or σ_i, or both. Keeping n_i constant, we select three different values of σ_i, $\sigma_i = 0$, 0.5, and 1, in our simulation. It should be noted that even for $\sigma_i = 0$, i.e., for

point impurity particles, the excluded area for occupation of active-particle centers is nonzero.

III. RESULTS AND DISCUSSIONS

We first study the influence of mobile impurity for the lattice CP in two dimensions. We then focus our study on the critical behavior of the continuum CP.

A. Lattice CP with mobile impurity

The primary purpose of this work is to examine if the effect of mobile impurity for the 2D lattice CP is qualitatively similar to that in one dimension. We carried out MC simulations for the two selected values of w, $w = 0.5$ and 1.0, with $n_i = 0.2$. The higher value of w implies the more frequent hopping that corresponds to higher diffusion velocity. The control parameter of the model is apparently λ; however, in the simulations we employed $p_\lambda = \frac{\lambda}{1+\lambda}$ in the Secs. III A through III C and λ in Sec. III D. To avoid complexity caused by using equivalent parameters, we converted the values of p to the λ values.

Plotted in Fig. 2 are the data of $\rho(t)$ for (a) $w = 0.5$ and (b) $w = 1.0$. The data in each plot decay rapidly for $\lambda < \lambda_c$ and saturate for $\lambda > \lambda_c$, with the critical values $\lambda_c = 2.057\,36(13)$ for $w = 0.5$ and $\lambda_c = 2.052\,41(9)$ for $w = 1.0$, at which $\rho(t)$ decreases following the power-law behavior

$$\rho(t) \sim t^{-\delta} \tag{1}$$

with the decay exponents $\delta = 0.583(3)$ and 0.541(3) for $w = 0.5$ and 1.0, respectively. From the plots, it is evident that the two data sets are qualitatively similar and appear to exhibit an ordinary critical behavior; however, the decay exponents are considerably larger than that of the clean CP, $\delta_0 = 0.451$, in both cases. Although the two values differ by less than 10%, the difference is clearly beyond error tolerance. The values of λ_c for the two cases are also similar but not the same (see below). For the larger w value, the exponent becomes smaller and closer to the clean CP value. In principle, higher w corresponds to higher diffusion rate of D in Ref. [34], where the value of δ decreased as D increased and converged to the clean CP value in the $D \to \infty$ limit; thus our observation is qualitatively consistent with that in one dimension. Therefore, mobile impurity indeed affects the critical behavior in such a way that it smears the nonuniversal power-law behavior. The source of nonuniversal power laws in the Griffiths phase has been attributed to the competition of spreading and extinction of active particles in the confined area surrounded by impurities, and mobility of impurities appeared to break up such confinement.

It is worth emphasizing that the supercritical data of $\rho(t)$ reach a minimum before saturation for λ close to λ_c. Similar undershooting has been observed for the Manna sandpile model [37,38], where such behavior was attributed to the initial random distribution of active particles. When dynamics began with uniform or hyperuniform [39] distribution of active particles, such undershooting was eliminated. In the CP with impurity, the initial distribution of active particles is nonuniform because of randomly distributed impurity particles. As time evolves, the system appears to reach an optimal distribution at which $\rho(t)$ becomes minimal and, after a transient time, the distribution becomes hyperuniform by consecutive spreading and extinction processes. It might be interesting to investigate how the distribution of active particles varies as time evolves. We will leave it for a future work.

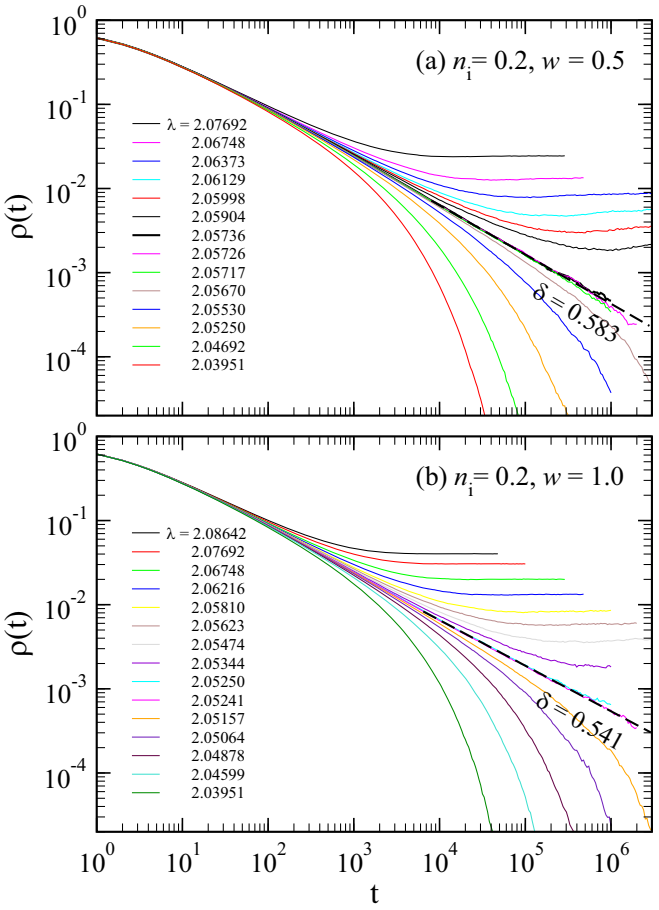

FIG. 2. Data of $\rho(t)$ for the CP with mobile impurity on a square lattice of a linear size $L = 2000$, calculated using the impurity density $n_i = 0.2$ and hopping probabilities (a) $w = 0.5$ and (b) $w = 1.0$ for various values of λ. The dashed line in each plot is the power-law fit over the data at λ_c that yields the decay exponent $\delta = 0.583(3)$ for $w = 0.5$ and 0.541(3) for $w = 1.0$. The legends are of the same order as the data from top to bottom in both plots.

The order-parameter exponent β was calculated from the saturated values of $\rho(t)$ in the supercritical region, and the results are plotted in Fig. 3. Data for both w values show good power-law behaviors

$$\rho_{\rm sat}(\varepsilon) \sim \epsilon^{\beta}, \tag{2}$$

$\varepsilon \equiv \lambda - \lambda_c$ being the distance from criticality, using the value of λ_c obtained from Fig. 2. The exponent β was estimated to be $\beta = 0.921(8)$ and 0.878(5) for $w = 0.5$ and 1.0, respectively. As w increases, the exponent value β decreases and this trend is also consistent with that in one dimension [34], where β decreased as D increased. The plots in Fig. 3 also assure us that the values of λ_c for the two values of w differ from each other; the plot is sensitive enough such that any single value fails to yield both plots linear.

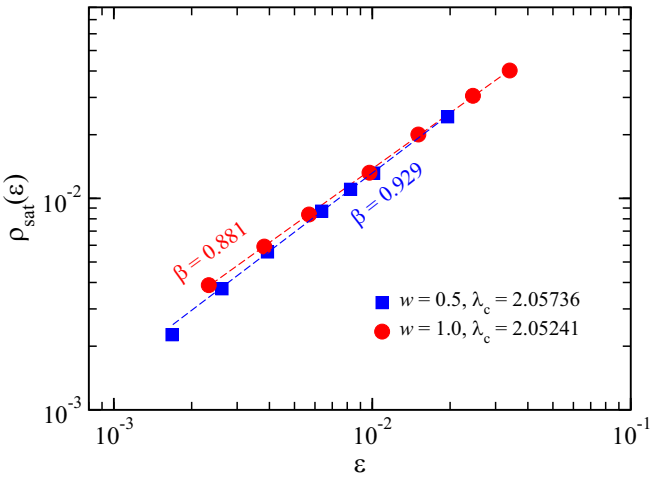

FIG. 3. Data of $\rho_{sat}(\varepsilon)$ calculated from the supercritical data of Fig. 2 for both $w = 0.5$ (blue circle) and 1.0 (red square) as a function of $\varepsilon = \lambda - \lambda_c$ on a double logarithmic scale. The dashed lines are the power-law fits, yielding $\beta = 0.921(8)$ and 0.878(5) for $w = 0.5$ and 1.0, respectively.

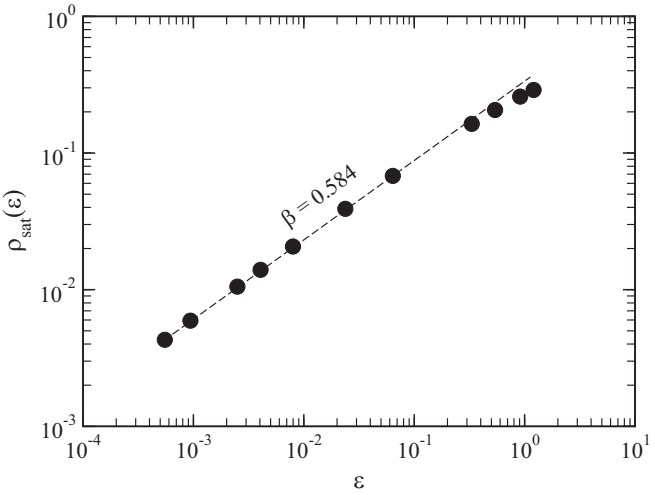

FIG. 5. Data of $\rho_{sat}(\varepsilon)$ calculated from the supercritical data in Fig. 4 as a function of $\varepsilon = \lambda - \lambda_c$ on a double logarithmic scale. The dashed line is the power-law fit using $\lambda_c = 1.793\,14$, yielding $\beta = 0.584(2)$.

B. CP in continuous media

We first carried out MC simulations for the clean CP to validate the proposed continuum model that should exhibit the DP critical behavior, With initial 4×10^6 particles in a system of $L = 2000$, dynamics proceeded up to 10^6 MC steps, and the data of $\rho(t)$ were sampled for selected values of λ. Results are plotted in Fig. 4. The best power-law behavior was observed at $\lambda_c = 1.793\,14$, with the power of $\delta = 0.451(2)$. The saturated density ρ_{sat} was also calculated from the supercritical data in Fig. 4, and the results were plotted as a function of ε in Fig. 5; an excellent power-law behavior was observed for the data close to the critical point (leftmost data), and the order-parameter exponent was estimated to be $\beta = 0.584(2)$. The four data points on the right end deviate from the power law apparently due to those data being far from criticality and out of the scaling region. The critical exponents δ and β are indeed close to the known values in the DP universality class [3]. We believe it to be sufficient to validate our continuum model and further analysis is therefore skipped.

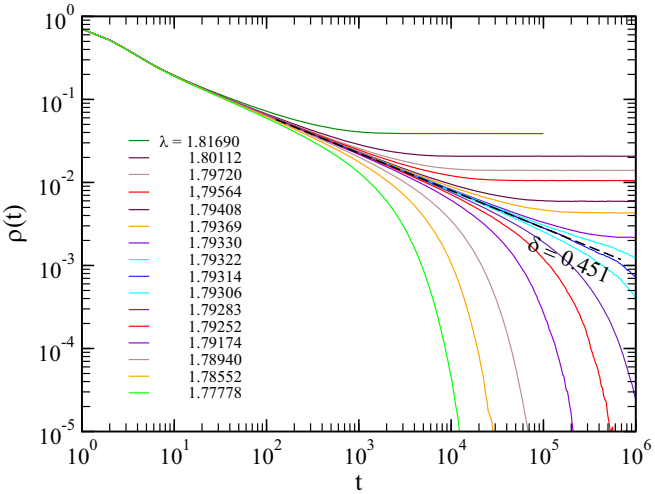

FIG. 4. Data of $\rho(t)$ for the clean continuum CP for selected values of λ. The legend shows the values of λ for the data set with the same order from top to bottom. The best power law was observed for $\lambda_c = 1.793\,14$ with the power of $\delta = 0.451(2)$.

C. Continuum CP with quenched impurity

The quenched disorder added to the lattice CP is known to yield the data for $\rho(t)$ nonuniversal power-law behaviors in the region between clean and dirty critical points, i.e., in the Griffiths phase of $\lambda_c^0 < \lambda < \lambda_c$, and an activated scaling at λ_c; the critical point is determined from the power-law plot of $\rho(t) \sim (\ln t)^{-\bar{\delta}}$ with $\bar{\delta} = \beta/(\nu_\perp \psi)$ [29,31]. Since an accurate determination of the critical point is a delicate task for the activated scaling, we here limit our work for the continuum CP with quenched impurity showing the nonuniversal power-law behaviors in the region of $\lambda > \lambda_c^0$.

Shown in Fig. 6 are the data of $\rho(t)$ calculated using (a) $\sigma_i = 0$ and (b) $\sigma_i = 1$ for selected values of λ. In (a), $\sigma_i = 0$ implies that impurities are point particles and active-particle centers cannot locate within an area of $\frac{1}{4}\pi$ centered on each of the impurity particles. In the plot, the data for $\lambda < 2.095\,98$ exhibit clear power-law behaviors, with the powers depending on the values of λ. For $\lambda = 2.095\,98$ data appear to be bent slightly upward; the plot of $\rho(t)$ against $\ln t$ on a double logarithmic scale indeed yields a linear behavior, indicating that the critical point is close to $\lambda = 2.096$ (not shown). An accurate determination of λ_c requires data of longer time steps, and it is the scope beyond this work. When the size of impurity particles is the same as that of active particles, i.e., $\sigma_i = 1$, the excluded area around each impurity particle is four times larger than that of (a). The data of $\rho(t)$ for $\lambda < 3.0$ show nonuniversal power-law behaviors and those for $\lambda = 3.0$ show slight upward bending. Indeed the data for $\lambda = 3.0$ plotted as a function of $\ln t$ show the power-law behavior, indicating that λ_c is close to 3.0. These results are qualitatively similar to

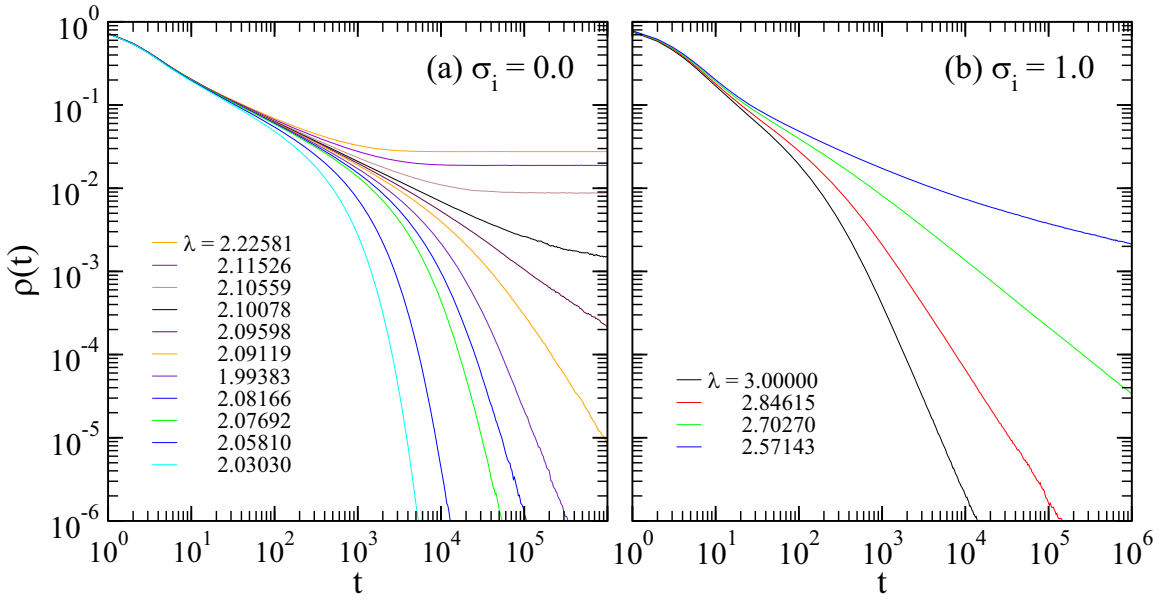

FIG. 6. Data of $\rho(t)$ for the continuum CP with quenched impurity using impurity disks of number density $n_i = 0.2$ and diameters (a) $\sigma_i = 0.0$ and (b) $\sigma_i = 1.0$ for selected values of λ. The legends are of the same order as the data from top to bottom in both plots.

those that were observed from the MC data for the disordered lattice CP [30]. We therefore confirm that the present continuum model exhibits the DP critical behavior and is distinct from the interacting particle model in [21].

D. Continuum CP with mobile impurity

We now present the main results of this paper, i.e., those for the CP with mobile impurity. Assuming that the area fraction excluded from active-particle centers is the impurity density, it is increased by varying the size of impurity particles, Simulations were carried out for three selected values of σ_i, $\sigma_i = 0$, 0.5, and 1.0. For $\sigma_i = 0$, i.e., for point impurities, sum of areas of diameter unity centered at all point impurities is the excluded area for active-particle centers to be created. For $\sigma_i > 0$, the impurity density is the area fraction of disks of diameter $1 + \sigma_i$ from all impurity particle centers, which is the area fraction of randomly distributed disks of diameter $1 + \sigma_i$ having an impenetrable core of diameter σ_i surrounded by the penetrable concentric shell of thickness $\frac{1}{2}$. Such an area fraction can be obtained from the early studies for the penetrable-concentric-shell model as [40]

$$\Phi = \eta - I_2\eta^2 + O(\eta^3), \tag{3}$$

where $\eta = n_i \frac{\pi}{4}(1+\sigma_i)^2$ is the reduce density and

$$I_2 = 2(1-k^2) - \frac{1}{\pi}\left[\frac{3\pi}{2} + (1-4k^2)\sin^{-1}k - 3k(1-k^2)^{1/2} + 2k(1-k^2)^{3/2}\right]$$

with the impenetrability parameter $k = \frac{\sigma_i}{1+\sigma_i}$. The low density expression in Eq. (3) was proved by computer simulation to give an excellent approximation even at high densities [41]. For $n_i = 0.2$, $(\eta, k) = (0.2\frac{\pi}{4}, 0)$ for $\sigma_i = 0$, $(0.2\frac{9\pi}{16}, \frac{1}{3})$ for $\sigma_i = 0.5$, and $(0.2\pi, \frac{1}{2})$ for $\sigma_i = 1$; therefore, $\Phi_i \simeq 0.145$, 0.319, and 0.523 for $\sigma_i = 0$, 0.5, and 1, respectively.

Simulation begins with $n_i L^2$ impurity particles distributed on the lattice sites chosen at random and $(1-n_i)L^2$ active particles on the rest of the sites on a square system of a linear size L. The critical spreading rate was determined from the power-law behavior of $\rho(t) \sim t^{-\delta}$ on a system of $L = 2000$, with 8×10^5 impurity particles and 3.2×10^6 initial active particles. With these particles, simulation requires extremely long computing time. If smaller systems are used, the simulation requires less computing time but more samples are required to reduce statistical fluctuations. In general, smaller system results in the finite-size effect and thus we prefer larger systems. We also carried out additional simulations on smaller systems of $L = 50$, 100, 200, 400, and 800 to investigate the finite-size effect.

Shown in Fig. 7 are the data of $\rho(t)$ for $\sigma_i = 0$ and selected values of λ on a double logarithmic scale. Data for $\lambda = 2.1050$ show reasonably good power-law behavior with the power of $\delta = 0.513(6)$. It should be noted that the accuracy of λ_c is limited to four decimal digits because of large computing time. Data for other values of λ deviate upward or downward, depending on whether the system is supercritical or subcritical. Thus, the CP with mobile impurity yields the usual power-law behaviors, unlike the case with quenched impurity. The decay exponent δ is estimated to be slightly larger than that of the clean CP, $\delta_0 \simeq 0.451$, indicating that mobile impurity suppresses creation of offspring and enhances decay of the density of active particles. The order-parameter exponent was also estimated from the saturated values of $\rho(t)$ in the supercritical region; the estimated exponent was $\beta = 0.76(1)$, as shown in the inset, which is considerably larger than that of the clean CP, $\beta_0 = 0.584(4)$.

In order to calculate the critical exponents associated with the finite-size effect, we analyze the data for various size

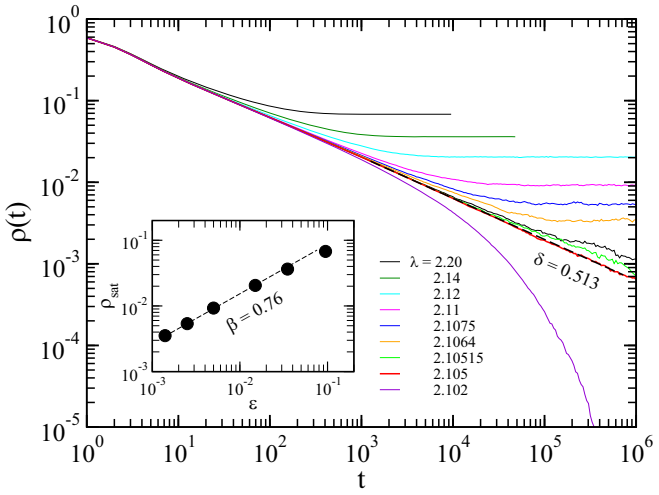

FIG. 7. Data of $\rho(t)$ for the continuum CP with mobile impurity, using the point impurities ($\sigma_i = 0$) of number density $n_i = 0.2$. The λ values of the data in the main panel are shown in the legend with the same order from top to bottom. The data exhibit usual power-law decay at $\lambda_c = 2.1050$. The dashed line on top of the data for λ_c is the power-law fit, yielding $\delta = 0.513(6)$. The inset is the steady-state density $\rho_{\rm sat}$ as a function of $\varepsilon \equiv \lambda - \lambda_c$, giving the exponent $\beta = 0.76(1)$.

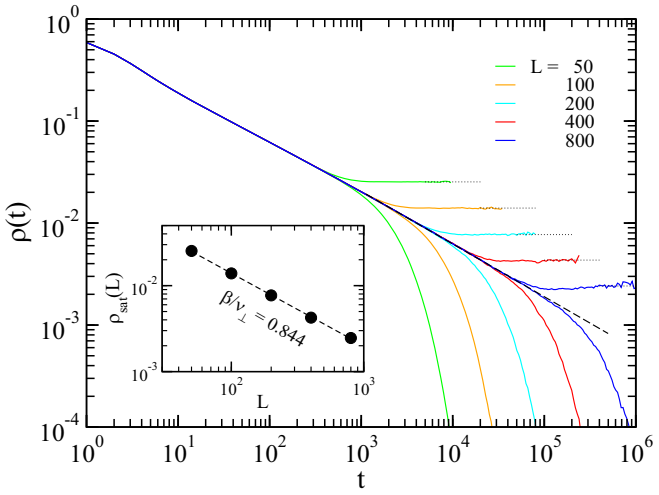

FIG. 8. Data of $\rho(t)$ at $\lambda_c = 2.1050$ for the continuum CP with mobile impurity, calculated using the point impurities ($\sigma_i = 0$) of $n_i = 0.2$. The decaying data are the all-sample averages and saturating data are the surviving-sample averages on systems of sizes, from top to bottom, $L = 50$, 100, 200, 400, and 800. Plotted in the inset are the data for $\rho_{\rm sat}$ as a function of L, with the power-law fit that gives the critical exponent $\beta/\nu_\perp = 0.844(5)$.

systems at criticality, using the scaling ansatz for the density of active particles,

$$\rho(t, \varepsilon, L) \equiv t^{-\delta} \mathcal{F}(t\varepsilon^{\nu_\parallel}, t/L^z), \tag{4}$$

where $\varepsilon = |\lambda - \lambda_c|$, and $\nu_\parallel$ and z are the temporal correlation-length exponent and dynamic exponent, respectively. One obtains that, in the supercritical region, $\rho(L \gg \xi) = \varepsilon^{\delta\nu_\parallel} = \varepsilon^\beta$ or, equivalently, $\beta = \delta\nu_\parallel$. On the other hand, for a finite system, because the spatial correlation length cannot exceed the system size, i.e., $\xi \sim |\varepsilon|^{-\nu_\perp} \sim L$ close to the criticality, one obtains that the temporal correlation length is given as $\tau \sim |\varepsilon|^{-\nu_\parallel} \sim \xi^{\nu_\parallel/\nu_\perp} \sim \xi^z$, i.e., $z = \frac{\nu_\parallel}{\nu_\perp}$. At the critical point of $\varepsilon = 0$, the steady-state density is a function of only L, i.e., $\rho_{\rm sat}(L) \sim L^{-\delta z} \propto L^{-\beta/\nu_\perp}$. Therefore the steady-state density plotted against the system size on a double logarithmic scale yields a power law behavior with the power of $-\beta/\nu_\perp$. Figure 8 shows the data of $\lambda_c = 2.1050$ on systems of linear sizes $L = 50$, 100, 200, 400, and 800; the saturating data are the averages over surviving samples up to time t and decaying data are the all-sample averages (averages over those samples that survive and fall into absorbing states). In the main panel, the data in the asymptotic region yield the power-law behavior $\rho(t) \sim t^{-\delta}$ (as marked with a dashed line) and, in the inset, the saturated densities $\rho_{\rm sat}$ (the values marked with dotted lines in the main panel) yield the power $\beta/\nu_\perp = 0.844(5)$.

We also calculated the quantity defined recently for surface roughening [42] and applied to the APT [43], given as

$$R(t, \varepsilon, L) = L\sqrt{\langle \rho(t)^2 \rangle / \langle \rho(t) \rangle^2 - 1}, \tag{5}$$

where $\langle \cdots \rangle$ indicates the average over samples. The quantity $R(t, \varepsilon, L)$ is associated with the moment ratio of the density of particles that was employed by Dickman [34]. In sufficiently large systems, the data of Eq. (5) are known to behave as $R(t) \sim t^{1/z}$ at criticality, and the saturated values in the supercritical region follow the power law$R_{\rm sat}(\varepsilon) \sim \varepsilon^{-\nu_\perp}$. Thus, the data of Eq. (5) give accurate estimates of the exponents z and $\nu_\perp$. Unfortunately, however, $R(t, \varepsilon, L)$ shows large statistical fluctuations unless the sample size is sufficiently large and, accordingly, accurate estimates of $R_{\rm sat}(\varepsilon)$ requires extremely long computing time. For this reason, we calculated the exponent z only. Figure 9 shows the data of $R(t, L)$ at criticality for five selected values of the system size L; the diverging data are

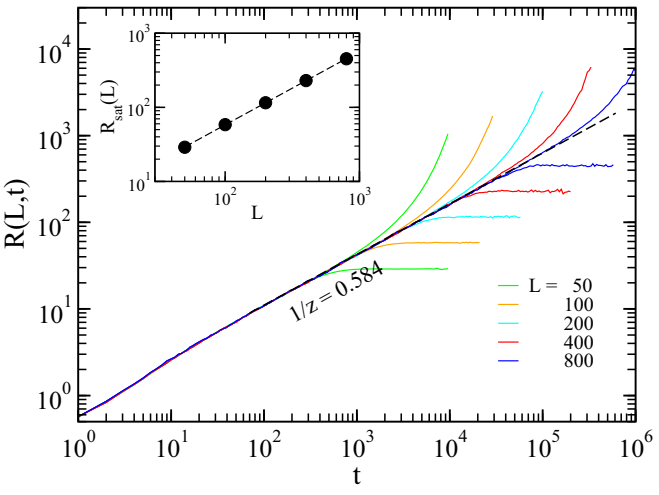

FIG. 9. Data of $R(L, t)$ for active-particle densities in the continuum CP with mobile impurity as a function of the evolution time, calculated using $n_i = 0.2$ and $\sigma_i = 0$. The diverging data in the main panel are the all-sample averages and the saturating data are the surviving sample averages on systems of sizes for, from top to bottom, $L = 50$, 100, 200, 400, and 800. The data in the inset are the steady-state values of $R_{\rm sat}(L)$, with the power of ≈ 1.

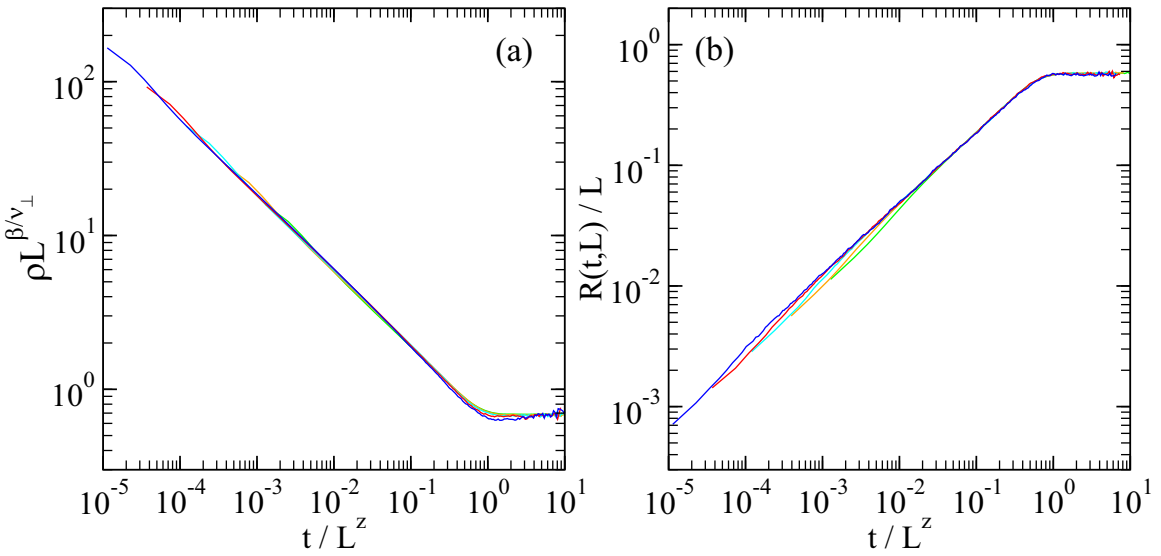

FIG. 10. Finite-size scaling data of (a) $\rho(t, L)$ and (b) $R(t, L)$, as a function of scaled time for the continuum CP with mobile impurity of $n_i = 0.2$ and $\sigma_i = 0.0$, using the measured values of the critical exponents, $\beta/\nu_\perp = 0.844$ and $1/z = 0.584$. The data for various size systems, i.e., for $L = 50$, 100, 200, 400, and 800, fall on the same curve.

the all-sample averages and saturating data are the surviving-sample averages. As the system size increases the power-law region becomes wider and, in the limit of $L \to \infty$, the data of $R(t)$ are expected to show the power-law behavior as marked with a dashed line, giving the power of $1/z = 0.584(5)$.

The estimates were confirmed by the finite-size scaling of $\rho(L, t) = L^{-\beta/\nu_\perp}\mathcal{G}(t/L^z)$ and $R(L, t) = LG(t/L^z)$ at criticality as shown in Fig. 10, where the data were scaled using the measured values of critical exponents.

Simulations for $\sigma_i = 0.5$ and 1.0 were also carried out, and the critical behavior was found to be qualitatively similar to that for $\sigma_i = 0$. Figure 11(a) shows the plot of $\rho(t)$ at criticality for selected values of σ_i; the critical spreading rates were estimated as $\lambda_c = 2.1050(3)$, 2.5311(1), and 3.1425(3), and the estimated decay exponents were $\delta = 0.513(6)$, 0.571(5), 0.624(5), for $\sigma_i = 0$, 0.5, and 1.0, respectively, As the size of impurity particles increases, the decay exponent increases, as expected. The order-parameter exponent β was also estimated using the saturated values $\rho_{\rm sat}(\varepsilon)$ in the $t \to \infty$ limit, and the results were $\beta = 0.76(1)$, 0.91(1), and 0.99(2), for $\sigma_i = 0$, 0.5, and 1, respectively, as shown in Fig. 11(b). It should be noted that the saturated values show downward curvatures as the distance from criticality increases, and the values of β were estimated from the data close to criticality. This deviation is not unusual and is natural because the power-law behavior of the order parameter holds near criticality and the distance from criticality $\varepsilon \equiv \lambda - \lambda_c \approx 0.1$ is quite large, and most data in this region are known

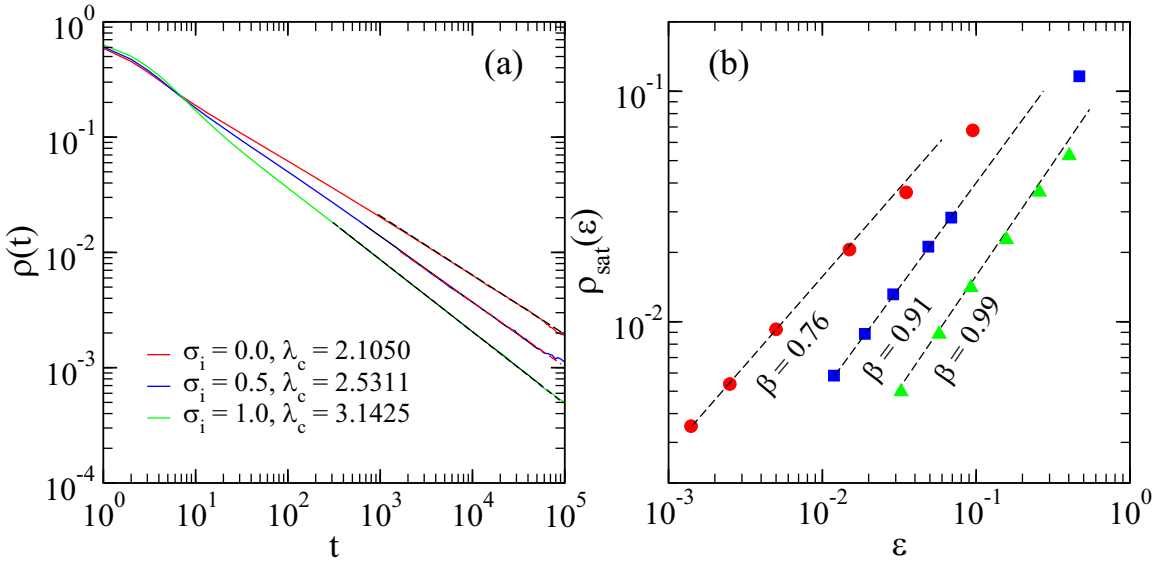

FIG. 11. Data for the continuum CP with mobile impurity of $n_i = 0.2$. Plotted in (a) are the data of $\rho(t)$ calculated at λ_c given in the legend. Data in (b) are the data of $\rho_{\rm sat}(\varepsilon)$ in the supercritical region. Both plots are for $\sigma_i = 0.0$, 0.5, and 1.0, from top to bottom.

TABLE I. Summary of the critical exponents for continuum CP with mobile impurity of number density $n_i = 0.2$. The first four exponents are those that were measured and the last two were calculated using the scaling relations.

σ_i	Φ	λ_c	δ	β	$\beta/\nu_\perp$	$1/z$	$\nu_\parallel$	$\nu_\perp$
0.0	0.145	2.1050(3)	0.513(6)	0.76(1)	0.844(5)	0.584(5)	1.48(4)	0.90(2)
0.5	0.319	2.5311(1)	0.571(5)	0.91(1)	0.885(2)	0.600(2)	1.59(3)	1.03(1)
1.0	0.523	3.1425(3)	0.624(5)	0.99(2)	0.942(5)	0.624(3)	1.59(4)	1.05(3)
clean CP	0.0	1.7931	0.451	0.584(4)	0.796	0.567	1.295(6)	0.734(4)

to deviate from the power law in the APT. More elaborate estimates will be attained if the data of $\rho_{\rm sat}$ are sampled for smaller values of ε; however, such work was not feasible in the present work.

The estimates of the critical exponents are summarized in Table I; the first four exponents are those that were directly measured from the MC data and the last two are those which were calculated using the scaling relations. It should be noted that the measured values of $1/z$ devaites by 5–8% from the values of $\nu_\perp/\nu_\parallel$. It is unclear if the differences were attributed to the violation of the scaling relation or are simply due to the inaccurate estimates of associated exponents that were used to estimate $\nu_\perp$ and $\nu_\parallel$. More extensive simulations are necessary to clarify the cause of such differences; however, we limited our work to the development of the continuum model and such work is beyond the scope of this work.

IV. SUMMARY AND CONCLUSIONS

We have studied by numerical simulations the critical behavior of the APT for lattice and continuum CPs with quenched and mobile impurities in two dimensions. Our primary aim was to examine whether the effect of mobile impurity on the critical behavior on a topologically different 2D lattice is qualitatively similar to that on a linear chain studied years ago by Dickman. On a 1D chain, impurity particles block the chains of active sites that participate activity and, as a result, active sites are finite and clustered, whereas in two and higher dimensions an infinite network of active sites always exists as long as the density of impurity particles is less than the percolation threshold. We found that despite the typological difference the critical behavior in two dimensions was qualitatively similar to that in one dimension, although the exponent values differed.

We also developed a continuum version of thr CP on a flat substrate without and with impurity. We first qualitatively examined the critical behaviors of a clean CP and a CP with quenched impurity. The impurity was assumed to be randomly distributed disks of diameter σ_i and number density $n_i = 0.2$. For the clean CP, the universal critical exponents were consistent with the corresponding lattice values, For the CP with quenched impurity, we observed nonuniversal power-law behaviors in the Griffiths phase of $\lambda_c^0 < \lambda < \lambda_c$ and activated scaling at λ_c for both $\sigma_i = 0$ and 1, where λ_c^0 and λ_c are the critical spreading rates of the clean CP and the CP with impurity, respectively. Our continuum model of the CP thus falls into the same universality class as the lattice CP.

The CP with mobile impurity was also studied, and the critical behavior was found to differ from that with quenched impurity but was found to show an ordinary critical behavior with the critical exponents differing from the DP values. As the hopping probability increased, the exponent became closer to the DP values. Although we were not able to observe whether the exponent values approach the clean-CP value as the hopping rate goes to infinity, our results are consistent with the general trend observed on a chain. It is also clear that, as the area fraction excluded from active-particle centers decreased, the exponents became close to the DP values. Thus, both the hopping probability of impurity particles and impurity density are relevant parameters that affect the critical behavior.

Our continuum model is purely a mathematical model that enables one to investigate the effect of impurity on the critical behavior in nonequilibrium phase transition. It can, however, readily be modified to the model of epidemic spreading such as that of COVID-19. For example, active particles are considered to be infected persons, impurity particles are recovered or immunized persons, and susceptible persons are anywhere in the space. When these persons form a crowd and mobile in a confined region, the spreading of epidemics might be examined with our model with some necessary modifications. Such a work might be an interesting topic for a future study.

ACKNOWLEDGMENTS

This work was supported by the National Research Foundation of Korea (NRF-2016R1A2B1013492), (NRF-2020R1A2C1003971) and by the Basic Science Research Program funded by the Ministry of Education (NRF-2021R1A6A1A03043957).

[1] J. Marro and R. Dickman, *Nonequilibrium Phase Transitions in Lattice Models* (Cambridge University Press, Cambridge, 1999).
[2] D. Ben-Avraham and S. Havlin, *Diffusion and Reaction in Fractals and Disordered Systems* (Cambridge University Press, Cambridge, 2000).
[3] H. Hinrichsen, Adv. Phys. **49**, 815 (2000).
[4] G. Ódor, Rev. Mod. Phys. **76**, 663 (2004).
[5] T. E. Harris, Ann. Probab. **2**, 969 (1974).
[6] P. Grassberger and A. de la Torre, Ann. Phys. (NY) **122**, 373 (1979).
[7] H. K. Janssen, Z. Phys. B **42**, 151 (1981).
[8] P. Grassberger, Z. Phys. B: Condens. Matter **47**, 365 (1982).
[9] W. Kinzel, Z. Phys. B **58**, 229 (1985).

[10] M. J. de Oliveira and J. E. Satulovsky, Phys. Rev. E **55**, 6377 (1997).
[11] I. Jensen, Phys. Rev. Lett. **70**, 1465 (1993); I. Jensen and R. Dickman, Phys. Rev. E **48**, 1710 (1993).
[12] P. Grassberger, F. Krause, and T. von der Twer, J. Phys. A **17**, L105 (1984); P. Grassberger, J. Phys. A: Math. Gen. **22**, L1103 (1989).
[13] H. Takayasu and A. Y. Tretyakov, Phys. Rev. Lett. **68**, 3060 (1992).
[14] S. S. Manna, J. Phys. A **24**, L363 (1991).
[15] M. Rossi, R. Pastor-Satorras, and A. Vespignani, Phys. Rev. Lett. **85**, 1803 (2000).
[16] N. Dees and S. Bahar, PLoS ONE **5**, e11952 (2010).
[17] H. Barghathi, S. Tackkett, and T. Vojta, Eur. Phys. J. B **90**, 129 (2017).
[18] D. J. Pine, J. P. Gollub, F. Grady, and A. M. Leshansky, Nature (London) **438**, 997 (2005).
[19] D. Fiocco, G. Foffi, and S. Sastry, Phys. Rev. E **88**, 020301(R) (2013).
[20] E. Tjhung and L. Berthier, Phys. Rev. Lett. **114**, 148301 (2015); J. Stat. Mech. (2016) 033501.
[21] S. B. Lee, J. Stat. Mech: Theory Exp. (2019) 053201.
[22] A. B. Harris, J. Phys. C **7**, 1671 (1974).
[23] P. G. de Gennes, *Scaling Concepts in Polymer Physics* (Cornell University Press, Ithaca, New York, 1979).
[24] A. J. Noest, Phys. Rev. Lett. **57**, 90 (1986); Phys. Rev. B **38**, 2715 (1988).
[25] R. B. Griffiths, Phys. Rev. Lett. **23**, 17 (1969).
[26] A. G. Moreira and R. Dickman, Phys. Rev. E **54**, R3090 (1996).
[27] R. Dickman and A. G. Moreira, Phys. Rev. E **57**, 1263 (1998).
[28] H. K. Janssen, Phys. Rev. E **55**, 6253 (1997).
[29] J. Hooyberghs, F. Iglói, and C. Vanderzande, Phys. Rev. Lett. **90**, 100601 (2003); Phys. Rev. E **69**, 066140 (2004).
[30] T. Vojta and M. Dickison, Phys. Rev. E **72**, 036126 (2005).
[31] T. Vojta, A. Farquhar, and J. Mast, Phys. Rev. E **79**, 011111 (2009).
[32] T. Senthil and S. Sachdev, Phys. Rev. Lett. **77**, 5292 (1996).
[33] J. M. Kim and S. B. Lee, Physica A **586**, 126464 (2022).
[34] R. Dickman, J. Stat. Mech.: Theory Exp. (2009) P08016.
[35] G. Evron, D. A. Kessler, and N. M. Shnerb, Physica A **389**, 428 (2010).
[36] M. E. Fisher, Phys. Rev. **176**, 257 (1968).
[37] M. Basu, U. Basu, S. Bondyopadhyay, P. K. Mohanty, and H. Hinrichsen, Phys. Rev. Lett. **109**, 015702 (2012).
[38] S. B. Lee, Phys. Rev. E **89**, 060101(R) (2014); **89**, 062133 (2014).
[39] S. Torquato and F. H. Stillinger, Phys. Rev. E **68**, 041113 (2003).
[40] S. Torquato, J. Chem. Phys. **81**, 5079 (1984); **83**, 4776 (1985); **84**, 6345 (1986).
[41] S. B. Lee and S. Torquato, J. Chem. Phys. **89**, 3258 (1988).
[42] J. M. Kim, J. Stat. Mech.: Theory Exp. (2021) 033213; J. Korean Phys. Soc. **81**, 602 (2022).
[43] J. M. Kim and S. B. Lee, Phys. Rev. E **105**, 025307 (2022).